Pergamon

0306-4549(94)00083-2

Ann. Nucl. Energy Vol. 22, No. 7, pp. 421–440, 1995

0306-4549/95 $9.50 + 0.00

SOLUTION OF 1-D MULTI-GROUP TIME-DEPENDENT DIFFUSION EQUATIONS USING THE COUPLED REACTORS THEORY

Y. NAGAYA[1] and K. KOBAYASHI[2]

[1]Japan Atomic Energy Research Institute, Tokai, Ibaraki, 319-11, Japan
[2]Department of Nuclear Engineering, Kyoto University,
Yoshida, Sakyo-ku, Kyoto 606, Japan

(Received 30 September 1994)

Abstract—A new method to solve time-dependent multi-group diffusion equations is presented using multi-point kinetics equations of the coupled reactors theory. The usual improved quasi-static method is generalized such that the fission sources for each core or node obtained from multi-point kinetics equations are used as amplitude functions for each node instead of a single amplitude function. Coupling coefficients between nodes were calculated exactly, and we found that the solution for a benchmark problem was in good agreement with the reference solution. It is shown that weakly coupled reactors of two cores can be well treated by a two-point model with constant coupling coefficients.

1. INTRODUCTION

A coupled reactors theory was firstly developed by Avery (1958), and his theory has been widely used to analyze coupled reactors and the strength of coupling between cores or nodes in large reactors (McFarlane et al. 1984; Brumbach et al. 1988). Although Avery gave the explicit form of the coupling coefficients, they were given from a physical intuition, and then his kinetics equations are valid only approximately (Komata 1969).

Recently, nodal kinetics equations for coupled reactors, namely, multi-point reactor kinetics equations whose dependent variables are fission sources in each node or core are derived rigorously (Kobayashi 1991, 1992). These equations are exact, independent of the strength of coupling between nodes. Thus we can apply them not only to coupled reactors but also to a reactor dividing it into several appropriate nodes.

These multi-point kinetics equations can be regarded as the generalization of the conventional one-point reactor kinetics equations. The main purpose of this paper

is to show that the solution of time-dependent diffusion equations can be obtained using these multi-point kinetics equations of the coupled reactors theory.

In the usual improved quasi-static (IQS) method (Ott and Menely 1969), the neutron flux is factorized into a rapidly varying amplitude function which is obtained by solving the conventional one-point reactor kinetics equations with a short time step and a slowly varying time-dependent shape function which is obtained by solving a static diffusion equation with a large time step.

This IQS method is extended in the present work such that fission sources for each core or node obtained from the multi-point kinetics equations are used as amplitude functions for each node instead of a single amplitude function. The shape functions are not calculated explicitly from the diffusion equation, because they are not continuous at the node boundary and boundary conditions for them are not simple. Instead of that, the neutron flux is calculated from the static diffusion equation by making use of the advantage that the shape functions change slowly in time.

In the present method, the amplitude function has the physical meaning of fission source contrary to the usual IQS method, where the amplitude function has no definite physical meaning if the weighting function is not unity (Henry 1975).

Multi-point kinetics equations are introduced in Chapter 2. The numerical method to solve the time-dependent diffusion equation using multi-point kinetics equations and the IQS method are given in Chapter 3. Numerical results are shown for a benchmark problem and for loosely coupled cores in Chapter 4. It is shown that weakly coupled reactors of two cores can be well treated by a two-point model with constant coupling coefficients.

2. MULTI-POINT REACTOR KINETICS EQUATIONS

We assume that a reactor described by the following static multi-group diffusion equation

$$A\phi_g(\boldsymbol{r}) = \frac{1}{k_0} B\phi_g(\boldsymbol{r}), \tag{1}$$

is critical with a criticality factor k_0 at $t < 0$, where the diffusion and fission operators A and B are defined by

$$A\phi_g(\boldsymbol{r}) = (-\nabla \cdot D_g \nabla + \Sigma_{rg})\phi_g(\boldsymbol{r}) - \sum_{g' \neq g} \Sigma_s(g \leftarrow g')\phi_{g'}(\boldsymbol{r}), \tag{2}$$

$$\text{with} \quad \Sigma_{rg} = \Sigma_{ag} + \sum_{g' \neq g} \Sigma_s(g' \leftarrow g), \tag{3}$$

and

$$B\phi_g(\boldsymbol{r}) = \chi_g F\phi_g(\boldsymbol{r}), \quad F\phi_g(\boldsymbol{r}) = \sum_{g'} \nu\Sigma_{fg'}(\boldsymbol{r})\phi_{g'}(\boldsymbol{r}), \tag{4}$$

respectively. $\phi_g(\boldsymbol{r})$ is the neutron flux of g-th group at the position $\boldsymbol{r}$, D_g the diffusion coefficient, Σ_{rg} the removal cross section, $\Sigma_s(g \leftarrow g')$ the scattering cross section from the g'-th group to the g-th group, Σ_{ag} the absorption cross section, $\nu\Sigma_{fg}$ the fission cross section multiplied by the number of fission neutrons, χ_g the fission neutron spectrum which can be space dependent. We use the zero flux boundary condition at the outer boundary of the whole reactor.

We assume that a step perturbation is introduced to the reactor in a steady state at $t = 0$, and the operators change as

$$A' = A + \delta A, \quad B' = B + \delta B, \quad F' = F + \delta F. \tag{5}$$

Then we assume that the flux changes according to the following time-dependent diffusion equations with delayed neutrons,

$$\frac{1}{v_g}\frac{\partial \phi_g(\boldsymbol{r},t)}{\partial t} = \left(-A' + \frac{1}{k_0}(1-\beta)B^{P\prime}\right)\phi_g(\boldsymbol{r},t) + \sum_i \chi_{ig}^d \lambda_i C_i(\boldsymbol{r},t), \tag{6}$$

$$\frac{\partial C_i(\boldsymbol{r},t)}{\partial t} = \frac{1}{k_0}\beta_i F'\phi_g(\boldsymbol{r},t) - \lambda_i C_i(\boldsymbol{r},t), \tag{7}$$

which are equations to be solved. Here, B^p is the fission operator for prompt neutrons defined by

$$B^P\phi_g(\boldsymbol{r},t) = \chi_g^P F'\phi_g(\boldsymbol{r},t) = \chi_g^P \sum_{g'} \nu\Sigma'_{fg'}(\boldsymbol{r})\phi_{g'}(\boldsymbol{r},t). \tag{8}$$

$\phi_g(\boldsymbol{r},t)$ is the time-dependent neutron flux and $C_i(\boldsymbol{r},t)$ the precursor density of the i-th delayed neutron group, v_g the mean neutron velocity of the g-th group. χ_g^p and χ_{ig}^d are the prompt and delayed neutron spectra, respectively, and λ_i and β_i are the decay constant and the delayed neutron fraction of the i-th delayed neutron group respectively. β is the sum of β_i.

The multi-point kinetics equations for Eqs.(6) and (7) are written in the form (Kobayashi 1992),

$$\begin{aligned} l_m(t)\frac{d}{dt}S_m(t) = &-\left(1 - \Delta k_m^F(t)\right)S_m(t) \\ &+ \sum_{n=1}^{N}\left[\frac{1}{k_0}\left(1-\beta_{mn}(t)\right)k_{mn}^p(t) - \Delta k_{mn}^A(t)\right]S_n(t) + \sum_{n=1}^{N}\sum_i \lambda_i k_{imn}^d(t)C_{in}(t), \end{aligned} \tag{9}$$

$$\frac{d}{dt}C_{im}(t) = -\lambda_i C_{im}(t) + \frac{1}{k_0}\beta_{im}S_m(t), \tag{10}$$

where $S_m(t)$ is the number of fission neutrons produced in the m-th core or node at time t, namely

$$S_m(t) = \int_{V_m} S(\boldsymbol{r},t)d\boldsymbol{r} = \int_{V_m} F'\phi_g(\boldsymbol{r},t)d\boldsymbol{r}. \tag{11}$$

V_m means the m-th core or node in a reactor dividing it into appropriate N nodes. $C_{im}(t)$ is the number of precursors of i-th delayed neutron group in the m-th node at time t,

$$C_{im}(t) = \int_{V_m} C_{im}(\boldsymbol{r}, t) d\boldsymbol{r}. \tag{12}$$

$k^p_{mn}(t)$ and $k^d_{imn}(t)$ are the coupling coefficients for prompt and delayed neutrons defined by

$$k^p_{mn}(t) = \frac{\int_{V_n} d\boldsymbol{r} \sum_g G_m(\boldsymbol{r}, g) \chi^p_g F' \phi_g(\boldsymbol{r}, t)}{\int_{V_n} d\boldsymbol{r} F' \phi_g(\boldsymbol{r}, t)}, \tag{13}$$

$$k^d_{imn}(t) = \frac{\int_{V_n} d\boldsymbol{r} \sum_g G_m(\boldsymbol{r}, g) \chi^d_{ig} C_i(\boldsymbol{r}, t)}{\int_{V_n} d\boldsymbol{r} C_i(\boldsymbol{r}, t)}, \tag{14}$$

respectively. $\Delta k^A_{mn}(t)$ and $\Delta k^F_m(t)$ correspond to the direct change of the coupling coefficients due to the perturbation of diffusion and fission operators defined by

$$\Delta k^A_{mn}(t) = \frac{\int_{V_n} d\boldsymbol{r} \sum_g G_m(\boldsymbol{r}, g) \delta A \phi_g(\boldsymbol{r}, t)}{\int_{V_n} d\boldsymbol{r} F' \phi_g(\boldsymbol{r}, t)}, \tag{15}$$

$$\Delta k^F_m(t) = \frac{\int_{V_m} d\boldsymbol{r} \delta F \phi_g(\boldsymbol{r}, t)}{\int_{V_m} d\boldsymbol{r} F' \phi_g(\boldsymbol{r}, t)}, \tag{16}$$

respectively. $l_m(t)$ is a kinetics parameter related to a generation time in the m-th node defined by

$$l_m(t) = \frac{\int_V d\boldsymbol{r} \sum_g G_m(\boldsymbol{r}, g) \frac{1}{v_g} \frac{\partial \phi_g(\boldsymbol{r}, t)}{\partial t}}{\int_{V_m} d\boldsymbol{r} \frac{\partial F' \phi_g(\boldsymbol{r}, t)}{\partial t}}. \tag{17}$$

$\beta_{mn}(t)$ and $\beta_{im}(t)$ are the parameters for the delayed neutrons defined by

$$\beta_{mn}(t) = \frac{\int_{V_n} d\boldsymbol{r} \sum_g G_m(\boldsymbol{r}, g) \beta \chi^p_g F' \phi_g(\boldsymbol{r}, t)}{\int_{V_n} d\boldsymbol{r} \sum_g G_m(\boldsymbol{r}, g) F' \phi_g(\boldsymbol{r}, t)}, \tag{18}$$

$$\beta_{im}(t) = \frac{\int_{V_m} d\boldsymbol{r} \beta_i F' \phi_g(\boldsymbol{r}, t)}{\int_{V_m} d\boldsymbol{r} F' \phi_g(\boldsymbol{r}, t)}, \tag{19}$$

respectively.

$G_m(\boldsymbol{r}, g)$ is the importance function defined by

$$A^\dagger G_m(\boldsymbol{r}, g) = \nu \Sigma_{fg}(\boldsymbol{r}) \delta_m(\boldsymbol{r}), \tag{20}$$

where $A^\dagger$ is the adjoint operator of the operator A of Eq.(2),

$$A^\dagger = -\nabla \cdot D_g \nabla + \Sigma_{rg} - \sum_{g' > g} \Sigma_s(g' \leftarrow g), \tag{21}$$

and $\delta_m(\boldsymbol{r})$ is a step function defined by

$$\delta_m(\boldsymbol{r}) = \begin{cases} 1, & \boldsymbol{r} \in V_m, \\ 0, & \boldsymbol{r} \notin V_m. \end{cases} \tag{22}$$

It is assumed that each node includes a fission source. This importance function must satisfy the same boundary conditions at the outermost boundary S of the reactor as for the flux of Eqs.(1) and (6), namely

$$G_m(\boldsymbol{r}, g) = 0 \quad \text{at } \boldsymbol{r} \in \mathrm{S}. \tag{23}$$

In the numerical solutions described in the next Chapter, appreciable numerical errors were found when calculating the kinetic parameter $l_m(t)$ by Eq.(17) using the finite difference approximation for the time derivative of neutron flux. In order to avoid these numerical errors, we reformulate the left hand side of Eq.(9) as

$$l_m(t)\frac{d}{dt}S_m(t) = \int_V d\boldsymbol{r} \sum_g G_m(\boldsymbol{r}, g)\frac{1}{v_g}\frac{\partial \phi_g(\boldsymbol{r}, t)}{\partial t} = \frac{d}{dt}(\hat{l}_m(t)S_m(t)), \tag{24}$$

where $\hat{l}_m(t)$ is defined by

$$\hat{l}_m(t) = \frac{\int_V d\boldsymbol{r} \sum_g G_m(\boldsymbol{r}, g)\frac{1}{v_g}\phi_g(\boldsymbol{r}, t)}{\int_{V_m} d\boldsymbol{r} F'\phi_g(\boldsymbol{r}, t)}. \tag{25}$$

In this formulation which does not contain any approximations, the parameter $\hat{l}_m(t)$ can be calculated without using the time derivative of the flux, and the numerical accuracy is improved.

3. APPLICATION OF THE IMPROVED QUASI-STATIC METHOD

In order to solve Eqs.(6) and (7), we apply an improved quasi-static method, which is slightly different from the ordinary one. Namely, we use the fission sources $S_m(t)$ for each node which are obtained from Eqs.(9) and (10) as amplitude functions.

We factorize the neutron flux into a node-dependent amplitude function $S_m(t)$ and a shape function $\psi_{mg}(\boldsymbol{r}, t)$ in node V_m as

$$\phi_g(\boldsymbol{r}, t) = S_m(t)\psi_{mg}(\boldsymbol{r}, t). \tag{26}$$

Applying the fission operator F' of Eq.(4) to Eq.(26), integrating it over node V_m and using the definition of Eq.(11), we can find that the shape function is normalized for each node as

$$\sum_{g'} \int_{V_m} \nu\Sigma'_{fg'}(\boldsymbol{r})\psi_{mg}(\boldsymbol{r}, t)d\boldsymbol{r} = 1, \tag{27}$$

which is independent of time.

Since the amplitude functions are different nodewise, the shape functions of Eq.(26) are not continuous at the interfaces between nodes. Therefore, it is difficult to calculate the shape function from the diffusion equation directly, because the boundary conditions for shape functions are not simple. However, we use the advantage that the change of the shape functions is slow, and use a larger time step width to calculate them in the finite difference approximation. Namely, we approximate the derivative of the shape function at time $t = t_{k+1}$ with a relatively large time step width $\Delta t_k = t_{k+1} - t_k$ as

$$\left.\frac{\partial}{\partial t}\psi_{mg}(\boldsymbol{r},t)\right|_{t=t_{k+1}} \approx \frac{\psi_{mg}(\boldsymbol{r},t_{k+1}) - \psi_{mg}(\boldsymbol{r},t_k)}{\Delta t_k}. \tag{28}$$

Using this approximation, the time derivative of Eq.(6) can be written as

$$\begin{aligned}
\left.\frac{\partial}{\partial t}\phi_g(\boldsymbol{r},t)\right|_{t=t_{k+1}} &= \left.\frac{dS_m(t)}{dt}\right|_{t=t_{k+1}} \psi_{mg}(\boldsymbol{r},t_{k+1}) + S_m(t_{k+1})\left.\frac{\partial}{\partial t}\psi_{mg}(\boldsymbol{r},t)\right|_{t=t_{k+1}} \\
&\approx \left.\frac{dS_m(t)}{dt}\right|_{t=t_{k+1}} \psi_{mg}(\boldsymbol{r},t_{k+1}) + S_m(t_{k+1})\frac{\psi_{mg}(\boldsymbol{r},t_{k+1}) - \psi_{mg}(\boldsymbol{r},t_k)}{\Delta t_k} \\
&= \frac{1}{S_m(t_{k+1})}\left.\frac{dS_m(t)}{dt}\right|_{t=t_{k+1}} \phi_g(\boldsymbol{r},t_{k+1}) \\
&\quad + \frac{1}{\Delta t_k}\left(\phi_g(\boldsymbol{r},t_{k+1}) - \frac{S_m(t_{k+1})}{S_m(t_k)}\phi_g(\boldsymbol{r},t_k)\right).
\end{aligned} \tag{29}$$

Substituting Eq.(29) into Eq.(6), we obtain a static equation for the flux at $t = t_{k+1}$,

$$\begin{aligned}
&-\nabla\cdot D'_g\nabla\phi_g(\boldsymbol{r},t_{k+1}) + \left(\Sigma'_{rg} + \frac{1}{v_g\Delta t_s} + \frac{1}{v_g S_m(t_{k+1})}\left.\frac{dS_m(t)}{dt}\right|_{t=t_{k+1}}\right)\phi_g(\boldsymbol{r},t_{k+1}) \\
&\quad = (1-\beta)\chi_g^p\frac{1}{k_0}\sum_{g'}\nu\Sigma'_{fg'}(\boldsymbol{r})\phi_{g'}(\boldsymbol{r},t_{k+1}) + \frac{1}{v_g\Delta t_s}\frac{S_m(t_{k+1})}{S_m(t_k)}\phi_g(\boldsymbol{r},t_k) \\
&\qquad + \sum_i \chi_{ig}^d\lambda_i C_i(\boldsymbol{r},t_{k+1}).
\end{aligned} \tag{30}$$

Eq.(30) can be solved for the flux $\phi_g(\boldsymbol{r},t_{k+1})$ with the given flux at t_k, $\phi_g(\boldsymbol{r},t_k)$, $S_m(t_k)$, $S_m(t_{k+1})$, $dS_m(t)/dt|_{t=t_{k+1}}$ and $C_i(\boldsymbol{r},t_{k+1})$. This can be done using the usual static multi-group diffusion code, which is modified to include these terms.

As in the usual IQS method, use is made of three different time steps, a shortest time step Δt_j to integrate the multi-point kinetics equations of Eqs.(9) and (10) with Eq.(24), an intermediate time step Δt_l to calculate kinetics parameters of Eqs.(13)-(19) and a largest time step Δt_k at which the flux distribution is calculated by solving Eq.(30).

The whole calculations are performed as follows: First, the importance functions and the flux for a steady state are calculated by solving Eq.(20) and the criticality equation of Eq.(1), respectively. Using these importance functions, the flux and precursor density for the critical state, the kinetics parameters of Eqs.(13)-(19) are calculated. Using these kinetics parameters, fission sources are calculated by integrating the kinetics equations of Eqs.(9) and (10) with Eq.(24) till the largest time step Δt_k. At the time $t = t_k + \Delta t_k$, the flux is calculated from Eq.(30), and we recalculate the kinetics parameters using a new flux interpolated from the two fluxes at $t = t_k$ and $t = t_{k+1}$ and then the fission sources or we proceed to the next time step.

4. NUMERICAL RESULTS

4.1. BSS BENCHMARK PROBLEM

In order to examine the usefulness of the present method, a code was developed to solve the multi-point kinetics equations of Eqs.(9) and (10) using the method given by Volodka (1968), and Eq.(30) by the implicit finite difference method.

First, we carried out numerical calculations[†] for the ANL benchmark problem BSS-6-A2 (National Energy Software Center 1985) of one-dimensional infinite slab geometry given by Stacey (1985). The geometry consists of three regions as shown in Fig.1, and the parameters used are listed in Table 1. The core was perturbed from its critical state by decreasing linearly the thermal absorption cross section in region 1 by 1 % in 1.0 second. Then the cross section was kept constant until 4.0 second.

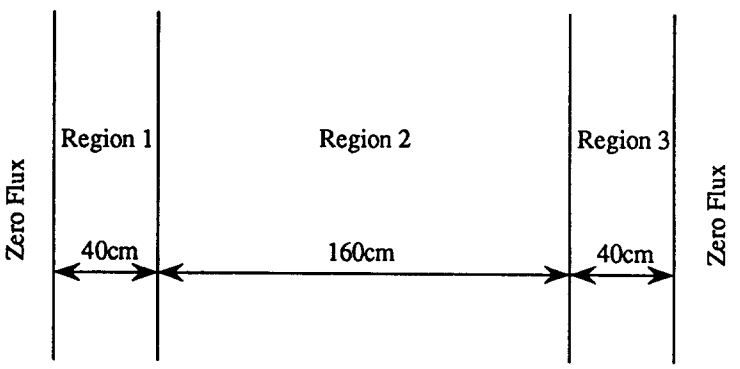

Fig.1 1-D infinite slab geometry of the ANL-BSS-6 benchmark problem

[†]Computations were performed by the FACOM M780 of the computation center of JAERI.

Table 1 Group constants for the 1-D ANL-BSS-6 benchmark problem

Constant	Region 1 and 3	Region 2
D_1(cm)	1.5	1.0
D_2(cm)	0.5	0.5
Σ_{r1}(cm^{-1})	0.026	0.02
Σ_{r2}(cm^{-1})	0.18	0.08
$\Sigma_{1\to2}$(cm^{-1})	0.015	0.01
$\nu\Sigma_{f1}$(cm^{-1})	0.01	0.005
$\nu\Sigma_{f2}$(cm^{-1})	0.2	0.099
χ_1	1.0	1.0
χ_2	0.0	0.0
v_1(cm/s)	1.0×10^7	1.0×10^7
v_2(cm/s)	3.0×10^5	3.0×10^5
Delayed Neutron Constants		
Group	$\overline{\beta_i}$	λ_i(sec^{-1})
1	0.00025	0.0124
2	0.00164	0.0305
3	0.00147	0.1110
4	0.00296	0.3010
5	0.00086	1.1400
6	0.00032	3.0100

The one-point model was used to solve this problem, namely, the multi-point kinetics equations of Eq.(9) with Eq.(24) for $N = 1$,

$$\frac{d}{dt}\left[\hat{l}_1(t)S_1(t)\right] = -(1-\Delta k_1^F(t))S_1(t) + \left(\frac{1}{k_0}(1-\beta_{11}(t))k_{11}^p(t) - \Delta k_{11}^A(t)\right)S_1(t) + \sum_i k_{i11}^d(t)\lambda_i C_{i1}(t), \tag{31}$$

was solved together with Eq.(10). Constant time step widths of $\Delta t_j = \Delta t_l$ =0.001sec were used to solve Eq.(31) with the coefficients calculated from Eqs.(12)-(19) and (25), and Δt_k =0.01sec to solve Eq.(30). The fast and thermal flux distributions obtained from Eq.(30) are shown in Figs.2 and 3, respectively.

The total power which is proportional to the total fission neutron source and is normalized to unity at $t = 0$ is shown in Fig.4 and Table 2 together with the reference values given by Stacey (1985). It can be seen that the total power obtained by the one-point model of the present method is in good agreement with the reference value through the whole time steps.

Next, we used the two-point model to solve the same problem. The core was divided into two nodes at the center of the core. The multi-point kinetics equations

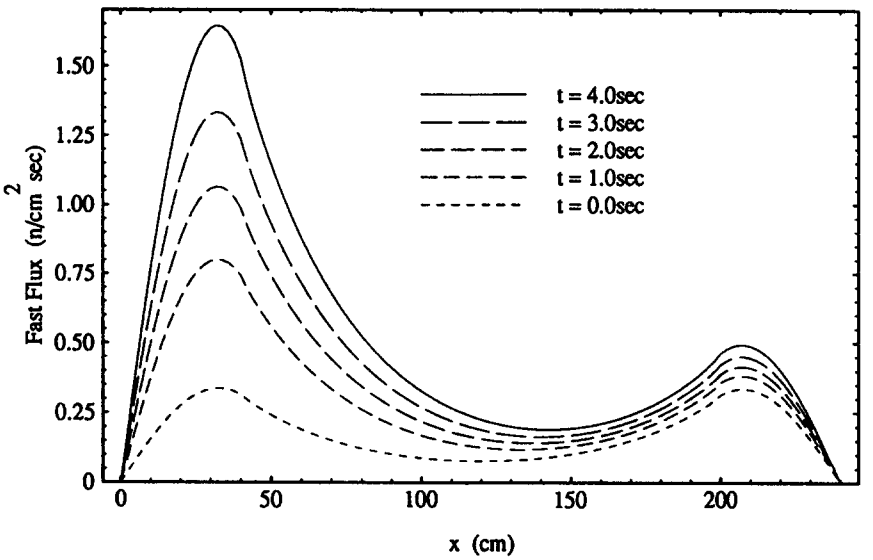

Fig.2 Flux distribution of the fast group for the 1-D ANL-BSS-6-A2 benchmark problem

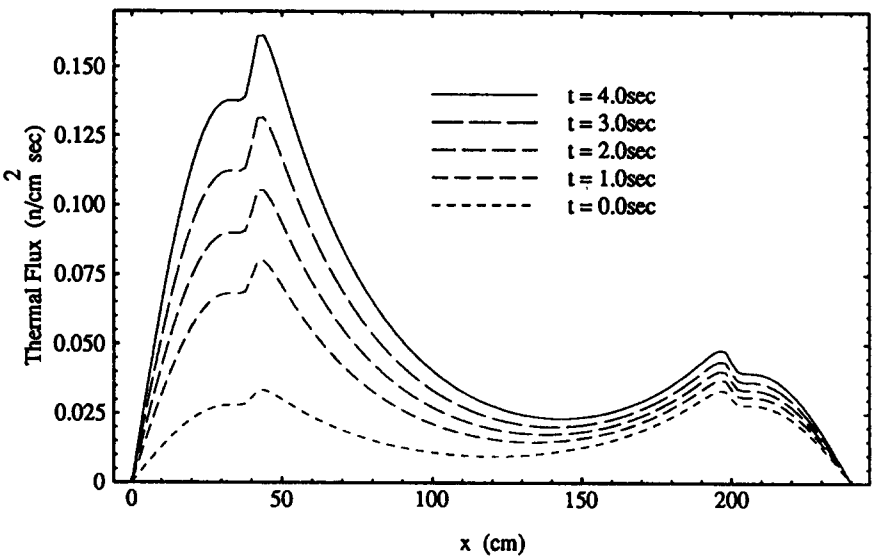

Fig.3 Flux distribution of the thermal group for the 1-D ANL-BSS-6-A2 benchmark problem

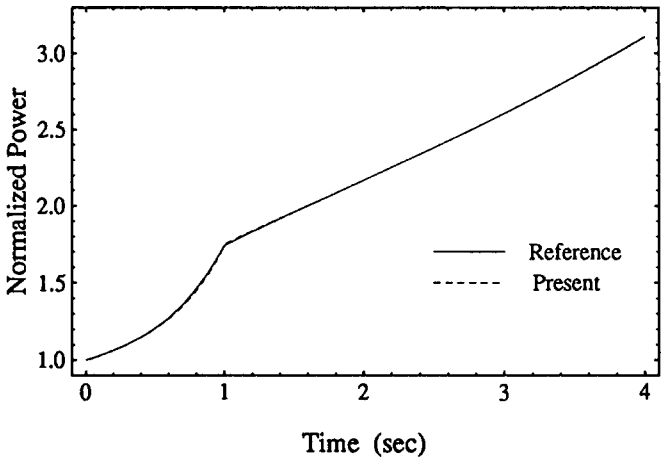

Fig.4 Total power calculated by the present method with one-point model and the reference value for the 1-D ANL-BSS-6-A2 benchmark problem

Table 2 Total power by the present method and the reference value for the 1-D ANL-BSS-6-A2 benchmark problem

	Reference	Present	
		1-point	2-point
Number of Meshes	120	120	120
Time Step (sec)	0.001	0.001‡	0.001‡
Total CPU Time (sec)		328	391
Time (sec)		Relative Power	
0.0	1.000	1.000	1.000
0.1	1.028	1.028	1.028
0.2	1.063	1.062	1.062
0.5	1.205	1.204	1.205
1.0	1.740	1.740	1.740
1.5	1.959	1.960	1.960
2.0	2.166	2.166	2.166
3.0	2.606	2.606	2.606
4.0	3.108	3.109	3.109
Regional Power Fractions at 4.0sec			
Region 1	0.4424	0.4424	0.4424
Region 2	0.4306	0.4306	0.4306
Region 3	0.1272	0.1271	0.1271

‡ time step size for amplitude functions

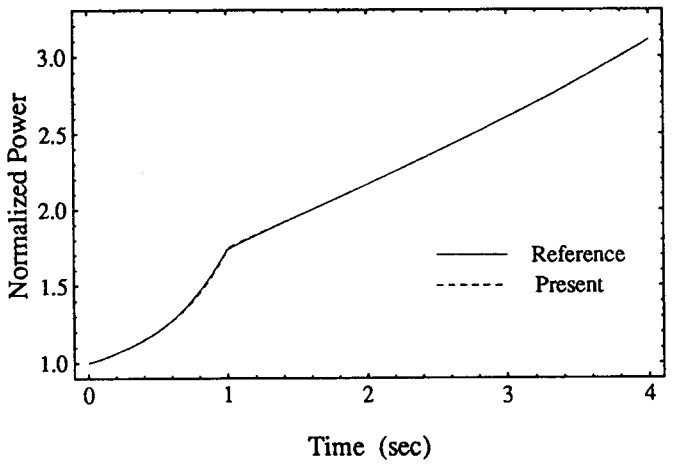

Fig.5 Total power calculated by the present method with two-point model and the reference value for the 1-D ANL-BSS-6-A2 benchmark problem

of Eq.(9) with Eq.(24) for $N = 2$,

$$\frac{d}{dt}\left[\hat{l}_1(t)S_1(t)\right] = -\left(1-\Delta k_1^F(t)\right)S_1(t) + \sum_{n=1}^{2}\left[\frac{1}{k_0}\left(1-\beta_{1n}(t)\right)k_{1n}^p(t) - \Delta k_{1n}^A(t)\right]S_n(t) + \sum_{n=1}^{2}\sum_i \lambda_i k_{i1n}^d(t)C_{in}(t), \quad (32)$$

$$\frac{d}{dt}\left[\hat{l}_2(t)S_2(t)\right] = -\left(1-\Delta k_2^F(t)\right)S_2(t) + \sum_{n=1}^{2}\left[\frac{1}{k_0}\left(1-\beta_{2n}(t)\right)k_{2n}^p(t) - \Delta k_{2n}^A(t)\right]S_n(t) + \sum_{n=1}^{2}\sum_i \lambda_i k_{i2n}^d(t)C_{in}(t), \quad (33)$$

were solved together with Eq.(10). The same time step widths as for the one-point model were used.

Figure 5 shows the total power calculated by the two-point model and its reference value. As is the case for one-point model, the total power calculated by two-point model is in good agreement with the reference value. Thus, we found that a reasonable solution could be obtained by the two-point model as well as by the one-point model.

4.2. COUPLED REACTORS OF TWO CORES

We applied the present method to loosely coupled cores to verify the adequacy of the present method. The geometry is shown in Fig.6, which was constructed in the KUCA (Kyoto University Critical Assembly) to measure the effective delayed neutron fraction (Itoh, Kobayashi et.al. 1993). The reactor was composed of two

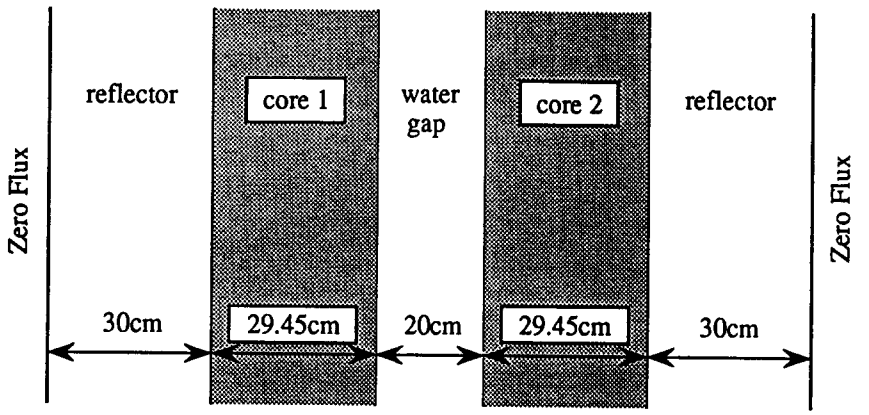

Fig.6 Geometry of coupled reactors of KUCA

Table 3 Two-group constants for the coupled reactors of KUCA

Constants	Core	Reflector
D_1(cm)	1.5432	1.2084
D_2(cm)	0.34309	0.14782
Σ_{a1}(cm^{-1})	2.5587×10^{-3}	4.8722×10^{-4}
Σ_{a2}(cm^{-1})	0.080477	0.018520
$\Sigma_{s1\to2}$(cm^{-1})	0.02201	0.058876
$\Sigma_{s2\to1}$(cm^{-1})	2.4407×10^{-4}	8.5534×10^{-5}
$\nu\Sigma_{f1}$(cm^{-1})	3.4164×10^{-3}	0.0
$\nu\Sigma_{f2}$(cm^{-1})	0.13933	0.0
χ_1	1.0	1.0
χ_2	0.0	0.0
v_1(cm/s)	1.95×10^7	1.95×10^7
v_2(cm/s)	2.2×10^5	2.2×10^5
$B_\perp^2$ (cm^{-2})	6.7494×10^{-3}	

Delayed Neutron Parameters		
Group	$\overline{\beta_i}$	λ_i(sec^{-1})
1	0.0002623	0.0124
2	0.0014703	0.0305
3	0.0012978	0.1110
4	0.0028098	0.3010
5	0.0008838	1.1400
6	0.0001796	3.0100

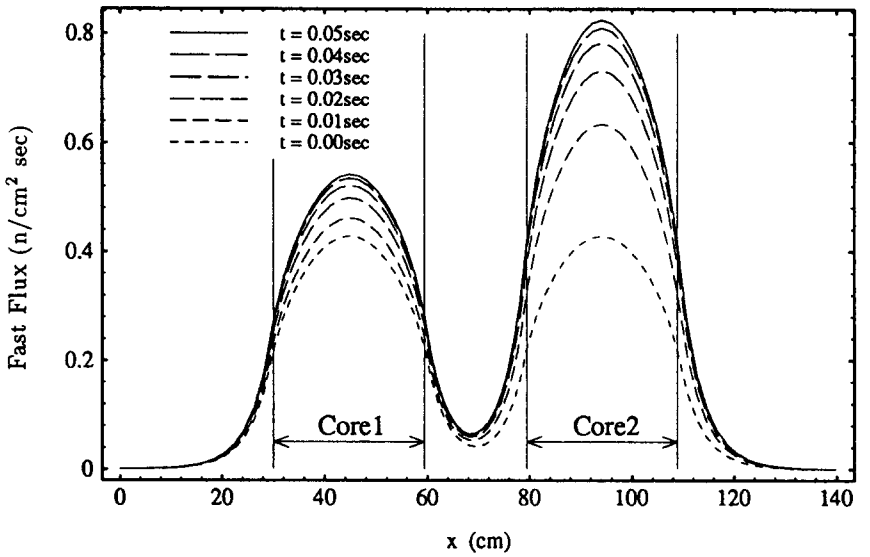

Fig.7 The flux distribution of the fast group at several time steps for the coupled reactors of two cores

cores, water gap and water reflectors. The width of the water gap between two cores was 20 cm.

We treated the reactor as two nodes whose boundary is at the center of water gap and solved the multi-point kinetics equations of Eq.(9) with Eq.(24) for $N = 2$. The left core is referred to as node 1 and the other node 2, which is symmetric. Namely, the composition of node 1 is the same as that of node 2 till the perturbation is introduced. Two group constants and delayed neutron data of six groups were calculated by the SRAC code (Tsuchihashi et. al. 1986), which are listed in Table 3.

A perturbation was introduced by decreasing the thermal absorption cross section of the core of node 2 by 0.5% stepwise at $t = 0$. In this problem, constant time step widths of $\Delta t_j = \Delta t_l = 0.0001$sec and $\Delta t_k = 0.002$sec which were fairly small, were used to calculate the prompt jump of the flux accurately due to the step perturbation.

Figures 7 and 8 show the change of the fast and thermal flux distributions, respectively. From these figures, it can be seen that the strength of the coupling between two cores is very weak and the flux distribution inside each core remains nearly unchanged.

Now we consider the coupling coefficients. We define the coupling coefficients k_{mn} as the mean value of k^p_{mn} and k^d_{imn},

$$k_{mn}(t) = \frac{1}{k_0}\left[(1-\beta)\,k^p_{mn}(t) + \sum_i \beta_i k^d_{imn}(t)\right]. \tag{34}$$

The coupling coefficient k_{mn} means the rate that a neutron, born in node n, produces

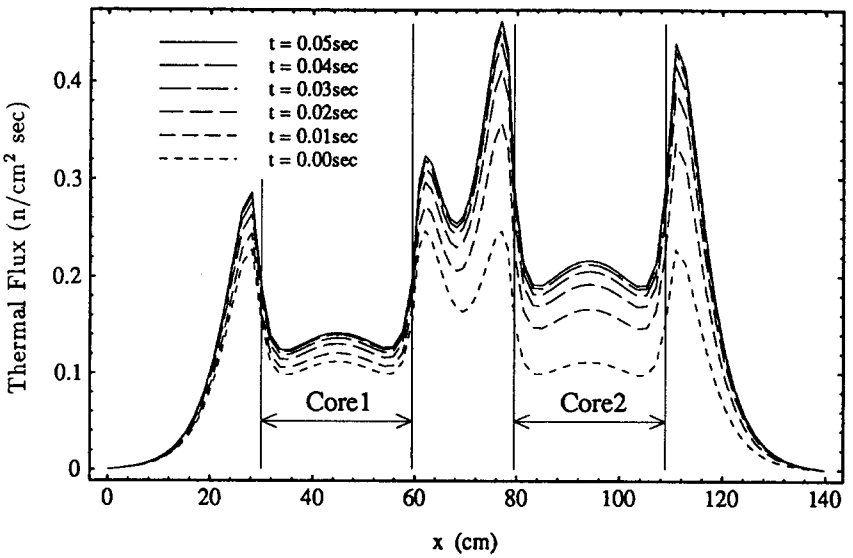

Fig.8 The flux distribution of the thermal group at several time steps for the coupled reactors of two cores

fission neutrons in node m in the next generation, whose change is not caused by the direct change of cross sections but the indirect change of flux distributions.

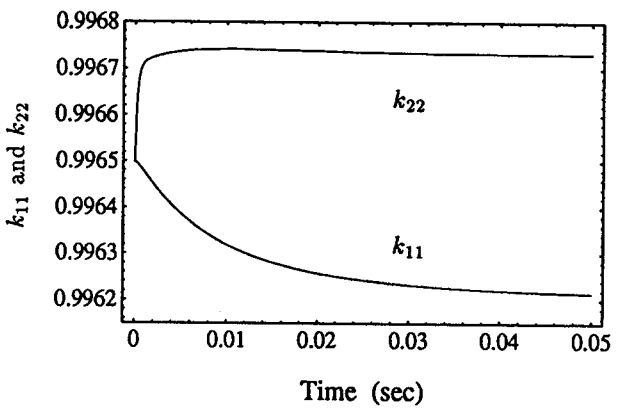

Fig.9 Temporal change of the coupling coefficients k_{11} and k_{22} for coupled reactors of two cores

Figure 9 represents the temporal change of coupling coefficients k_{11} and k_{22}. k_{22} for the perturbed node 2 increases rapidly after the step perturbation is introduced in node 2 at $t = 0$, and then it approaches to a constant value. On the other hand, k_{11} for the unperturbed node 1 decreases mildly and then it approaches a constant

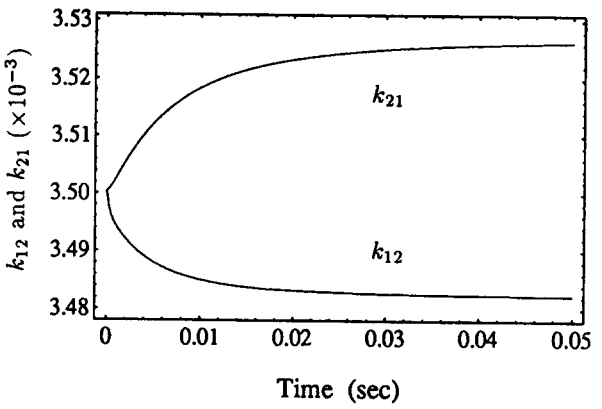

Fig.10 Temporal change of the coupling coefficients k_{12} and k_{21} for the coupled reactors of two cores

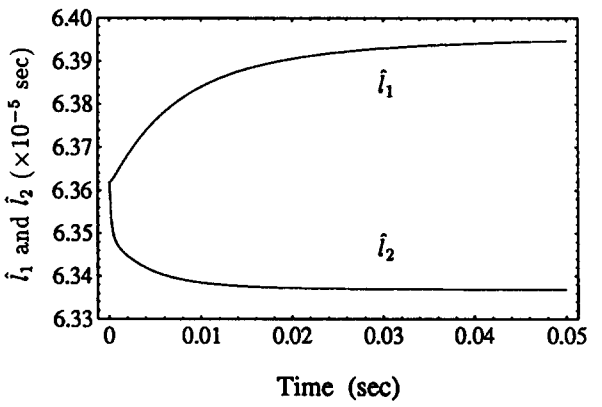

Fig.11 Temporal change of the kinetics parameters $\hat{l}_1$ and $\hat{l}_2$ for the coupled reactors of two cores

value. This is reasonable because there should be a delay before the perturbation in node 2 has the influence on the unperturbed node 1.

Figure 10 shows the temporal change of cross coupling coefficients k_{12} and k_{21}. Both coupling coefficients change in opposite directions gradually and afterwards they approach constant values. This implies that the number of the neutrons produced in node 2 by fissions induced by neutrons produced in node 1 increases and vice versa by a small spatial change of the flux distribution.

Figure 11 shows the temporal change of the kinetics parameters $\hat{l}_1$ and $\hat{l}_2$. The kinetics parameter $\hat{l}_2$ in the perturbed node 2 decreases rapidly after the perturbation is introduced. On the contrary, the kinetics parameter $\hat{l}_1$ in the unperturbed node 1 increases mildly.

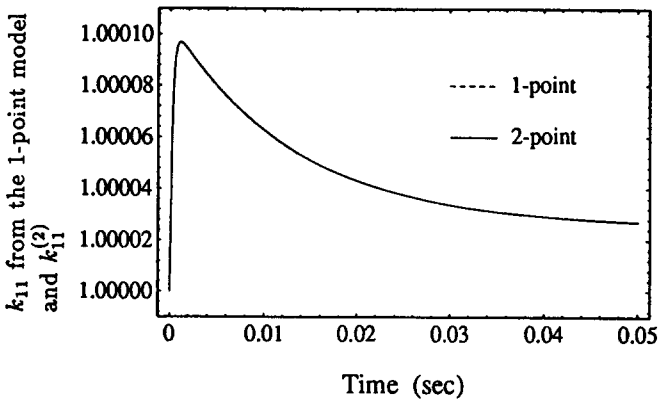

Fig.12 Coupling coefficients k_{11} obtained from the one- and two-point models

In order to confirm that the results obtained by the two-point model are consistent with those by the one-point model numerically, we also calculated the whole power and kinetics parameters by treating the reactor by the one-point model of $N = 1$. We can also calculate kinetics parameters for the one-point model by using those for the two-point model such that the kinetics equations for the two-point model are reduced to those for the one-point model.

We define the fission source $S_1^{(2)}(t)$ as the sum of the fission sources of two nodes $S_1(t)$ and $S_2(t)$ obtained by the two-point model as

$$S_1^{(2)}(t) = S_1(t) + S_2(t), \tag{35}$$

where the superscript (2) means that these values are calculated from the quantities obtained by the two-point model.

Adding the two kinetics equations of Eq.(32) and (33) for $N = 2$, and defining the averaged kinetics parameters as

$$\hat{l}_1^{(2)} = \frac{\left(\hat{l}_1 S_1(t) + \hat{l}_2 S_2(t)\right)}{(S_1(t) + S_2(t))}, \tag{36}$$

$$k_{11}^{p(2)} = (k_{11}^p + k_{21}^p)\frac{S_1(t)}{S_1(t) + S_2(t)} + (k_{12}^p + k_{22}^p)\frac{S_2(t)}{S_1(t) + S_2(t)}, \tag{37}$$

$$\Delta k_{11}^{A(2)} = \left(\Delta k_{11}^A + \Delta k_{21}^A\right)\frac{S_1(t)}{S_1(t) + S_2(t)} + \left(\Delta k_{12}^A + \Delta k_{22}^A\right)\frac{S_2(t)}{S_1(t) + S_2(t)}, \tag{38}$$

$$k_{i11}^{d(2)} = \left(k_{i11}^d + k_{i21}^d\right)\frac{C_{i1}(t)}{C_{i1}(t) + C_{i2}(t)} + \left(k_{i12}^d + k_{i22}^d\right)\frac{C_{i2}(t)}{C_{i1}(t) + C_{i2}(t)}, \tag{39}$$

we obtain a kinetics equation for $S_1^{(2)}(t)$ which has the same form as the kinetics equation of Eq.(31).

In Fig.12, the broken line shows the coupling coefficients k_{11} of Eq.(34) by the one-point model of $N = 1$ and the solid line the coupling coefficient $k_{11}^{(2)}$ derived from

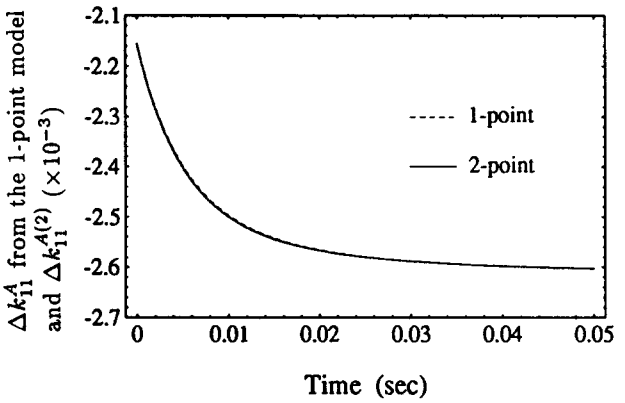

Fig.13 Coupling coefficients Δk_{11}^{A} obtained from the one- and two-point models

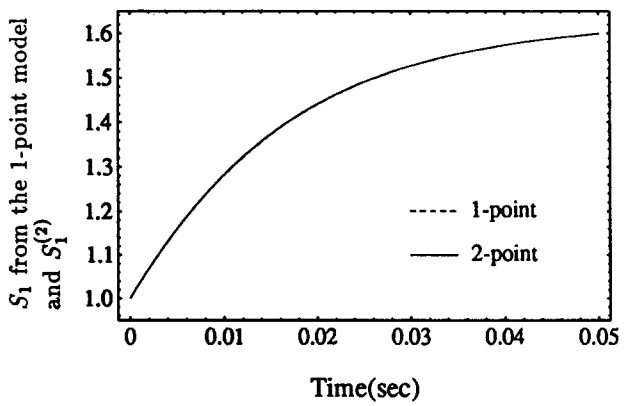

Fig.14 Total fission sources obtained from the one- and two-point models

the two-point model by substituting Eqs.(37) and (39) into Eq.(34), and we can see that both coupling coefficients are in good agreement. The increase of k_{21} and k_{22}, and the decrease of k_{11} and k_{12} caused a peak in $k_{11}^{(2)}$ which means a decrease of the multiplication rate of the whole reactor due to the change of the flux distribution immediately after the step perturbation was introduced. The coupling coefficients Δk_{11}^{A}, which is the contribution of the direct change of absorption cross section to the multiplication rate of the whole reactor, are compared in Fig.13. $\Delta k_{11}^{A(2)}$ obtained from the two-point model by Eq.(38) is in good agreement with that from the one-point model of $N = 1$. The kinetics parameters $\tilde{l}_1^{(2)}$, $k_{11}^{p(2)}$ and $k_{i11}^{d(2)}$ are also in good agreement with those for the one-point model though not presented.

In Fig.14 are compared the whole fission sources, $S_1^{(2)}(t)$ obtained from the two-point model by Eq.(35) and $S_1(t)$ from the one-point model, which are also in good agreement.

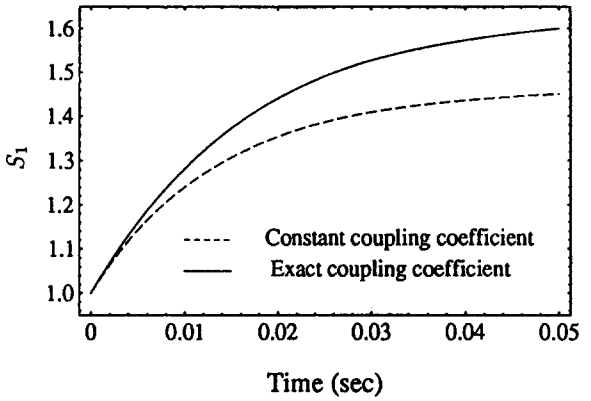

Fig.15 Total fission sources with constant coupling coefficients and the exact time-dependent coupling coefficients obtained by the one-point model

Good agreements of the above comparisons imply that the solution obtained from the two-point model is consistent with the one from the one-point model and the kinetics parameters including coupling coefficients are calculated accurately.

Finally, we made comparisons of fission sources calculated with constant coupling coefficients and the one with exact coupling coefficients to investigate the dependence of the fission source on coupling coefficients. In Fig.15, the solid line represents the exact fission source obtained from the coupling coefficients by calculating at each time step and the broken line shows the fission source calculated by assuming that the coupling coefficients remain constant at their initial values corresponding to those of the unperturbed reactor, both by the one-point model. This assumption is equivalent to the conventional point kinetics equation. The error in the fission source at $t = 0.05$sec is not small, -9.36% as shown in Table 4.

Table 4 Nodal fission sources at 0.05sec obtained using constant coupling coefficients and exact one

	One-point model		
	Exact coupling coefficients	Constant coupling coefficients	Error (%)
Node 1	1.5989	1.4493	−9.36
CPU time (sec)	9.07	0.22	
	Two-point model		
	Exact coupling coefficients	Constant coupling coefficients	Error (%)
Node 1	0.6339	0.6411	1.14
Node 2	0.9652	0.9299	−3.66
CPU time (sec)	12.78	0.46	

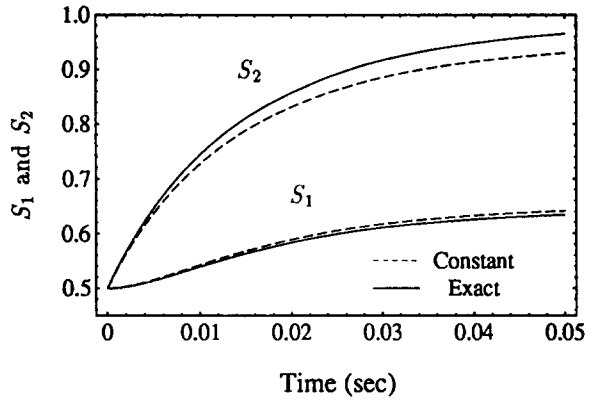

Fig.16 Total fission sources with the constant coupling coefficients and the exact coupling coefficients obtained from the two-point model with the perturbation of a 0.5% decrease of the absorption cross section

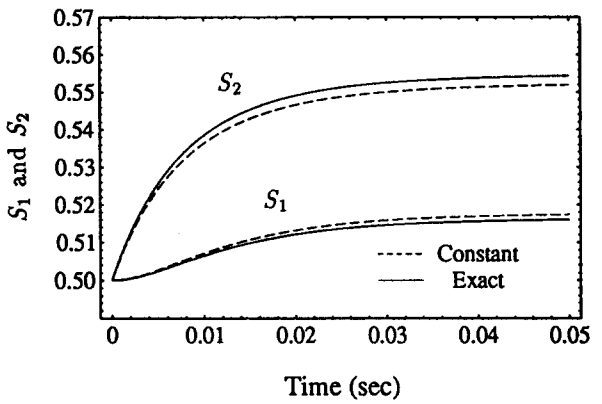

Fig.17 Nodal fission sources with the constant coupling coefficients and the exact coupling coefficients obtained by the two-point model with the perturbation of a 0.1% decrease of the absorption cross section

Figure 16 shows the fission sources in each node by the two-point model treating the cores as two nodes. In the case of the two point model, the fission source in node 1 at 0.05sec is overestimated by 1.14% and the one in node 2 is underestimated by 3.66% as shown in Table 4, when the coupling coefficients are assumed constant. The nodal fission sources obtained by assuming constant coupling coefficients are improved in the case of the two-point model, the error in the total fission source decreases to -1.76%.

Figure 17 shows the fission sources for the case of a small perturbation, where the absorption cross section was decreased by 0.1%. We can see that the fission sources

calculated using contant coupling coefficients agree better with the exact values than in the case of the larger perturbation of a 0.5% decrease in Fig.16.

Therefore, if the perturbation is small, and then the associated change of the coupling coefficients is also small, it is sufficient to use shape functions calculated without the perturbation throughout the whole transient period. In such a case, it is necessary only to solve the multi-point kinetics equations with constant coupling coefficients, and we can obtain the space-dependent solution efficiently. The extension of the present method to two- and three-dimensional problems is straightforward.

ACKNOWLEDGMENTS

The authors wish to express their sincere thanks to Dr. M. Nakagawa of Japan Atomic Energy Research Institute (JAERI) and Dr. E. Kiefhaber of Kernforschungszentrum Karlsruhe for their useful comments to the manuscript and to Dr. K. Tsuchihashi of JAERI for his support to this work.

REFERENCES

Avery R. (1958) "Theory of Coupled Reactors," *Proc. 2nd U.N. Int. Conf. Peaceful Use of Atomic Energy* **12**, 182.

Brumbach S.B., et al. (1988) *Nucl. Sci. Eng.*, **98**, 103.

Henry A., (1975) Nuclear-Reactor Analysis, The MIT Press, Chap.7.

Itoh H., Kobayashi K. et.al. (1993) Determination of the Effective Delayed Neutron Fraction Using the Coupled Reactors Theory II, Annual Meeting of the Atomic Energy Society of Japan, A12.

Kobayashi K. (1991) *Ann. Nucl. Energy* **18**, 13.

Kobayashi K. (1991) *J. Nucl. Sci. Technol.* **28**, 389.

Kobayashi K. (1992) *J. Nucl. Sci. Technol.* **29**, 110.

Komata M. (1969) *Nucl. Sci. Eng.* **38**, 193.

McFarlane H.F., Carpenter S.G., Collins P.J., Olsen D.N. and Brumbach S.B. (1984) *Nucl. Sci. Eng.*, **87**, 204.

Ott K.O. and Meneley D.A. (1969) *Nucl. Sci. Eng.*, **36**, 402.

Stacey Jr. W. M. (1985) Benchmark Problem Book, ANL-7416-Supplement 3., National Energy Software Center

Tsuchihashi, K., et al. (1986) Revised SRAC code system, JAERI-1302

Volodka L. K. (1968) ANL-7310, p492.